ResearchGate

See discussions, stats, and author profiles for this publication at: https://www.researchgate.net/publication/27313652

Multi-body dynamics in full-vehicle handling analysis

Article *in* Proceedings of the Institution of Mechanical Engineers Part K Journal of Multi-body Dynamics · January 2000

DOI: 10.1243/1464419991544027 · Source: OAI

CITATIONS
52

READS
1,581

3 authors:

Shahenaz Hegazy
University of Amsterdam
28 PUBLICATIONS **238** CITATIONS
SEE PROFILE

Homer Rahnejat
Loughborough University
434 PUBLICATIONS **4,923** CITATIONS
SEE PROFILE

Khalid Hussain
University of Wollongong in Dubai
30 PUBLICATIONS **378** CITATIONS
SEE PROFILE

Some of the authors of this publication are also working on these related projects:

Vibration energy harvesting from automotive powertrains View project

mixed non-Newtonian themo-elastohydrodynamics of hypoid gears View project

All content following this page was uploaded by Khalid Hussain on 26 May 2014.

The user has requested enhancement of the downloaded file.

Loughborough University

This item was submitted to Loughborough's Institutional Repository (https://dspace.lboro.ac.uk/) by the author and is made available under the following Creative Commons Licence conditions.

creative commons

COMMONS DEED

Attribution-NonCommercial-NoDerivs 2.5

You are free:

- to copy, distribute, display, and perform the work

Under the following conditions:

Attribution. You must attribute the work in the manner specified by the author or licensor.

Noncommercial. You may not use this work for commercial purposes.

No Derivative Works. You may not alter, transform, or build upon this work.

- For any reuse or distribution, you must make clear to others the license terms of this work.
- Any of these conditions can be waived if you get permission from the copyright holder.

Your fair use and other rights are in no way affected by the above.

This is a human-readable summary of the Legal Code (the full license).

Disclaimer

For the full text of this licence, please go to:
http://creativecommons.org/licenses/by-nc-nd/2.5/

Multi-body dynamics in full-vehicle handling analysis

S Hegazy, H Rahnejat* and **K Hussain**
Department of Mechanical Engineering, University of Bradford, West Yorkshire, UK

Abstract: This paper presents a multidegrees-of-freedom non-linear multibody dynamic model of a vehicle, comprising front and rear suspensions, steering system, road wheels, tyres and vehicle inertia. The model incorporates all sources of compliance, stiffness and damping, all with non-linear characteristics. The vehicle model is created in ADAMS (automatic dynamic analysis of mechanical systems) formulation. The model is used for the purpose of vehicle handling analysis. Simulation runs, in-line with vehicle manoeuvres specified under ISO and British Standards, have been undertaken and reported in the paper.

Keywords: multi-body dynamics, suspensions, steering, non-linear characteristics, simulations

NOTATION

a	distance from vehicle c.g. to the front tyre contact patch
b	distance from vehicle c.g. to the rear tyre contact patch
c	damping constant (tyre)
C_k	kth constraint function in a joint
dt	integration step size
F_{lat}	lateral tyre force
F_{long}	longitudinal tyre force
F_q	generalized forces in an Euler frame of reference
F_{vert}	vertical tyre force
f	coefficient of rolling resistance
g	gravitational acceleration
[J]	Jacobian matrix
k	tyre vertical stiffness
k_{lat}	tyre lateral stiffness
K	kinetic energy
l	axial length
m	number of constraints
M_X	overturning moment
M_Y	rolling resistance moment
M_Z	aligning moment
n	number of rigid parts
$\{\boldsymbol{q}\}^{\text{T}}$	generalized coordinates
s	a scaling factor
t	time
u	longitudinal speed
v	lateral speed
x, y, z	displacements in Cartesian coordinates
α	tyre slip angle
β	steer angle
γ	camber angle
δ	tyre deflection
λ	Lagrange multiplier
μ	coefficient of friction
ψ, θ, ϕ	Euler angles
ψ_{10}	vehicle body roll

Superscript

·	rate of change with time

Subscripts

f	front tyre
i, j	body i relative to body j
k	kth holonomic constraint function
r	rear tyre

The MS was received on 19 January 1999 and was accepted after revision for publication on 2 June 1999.
**Corresponding author: Department of Mechanical Engineering, University of Bradford, Bradford, West Yorkshire BD7 1DP, UK.*

1 INTRODUCTION

Multi-body dynamics has played an increasingly important role in the analysis of vehicle motions ever since the introduction of linear vehicle dynamic models by Segel [**1**] for lateral accelerations of up to 0.3 g. However, linear models include significant assumptions:

(a) small steering inputs at normal constant vehicle speeds,

(b) linear tyre behaviour with slip and camber angles,
(c) smooth flat roads and
(d) lateral tyre forces not altering with small changes in vertical tyre forces.

There are, in fact, many sources of non-linearity in suspension kinematics, steering characteristics, tyre properties and in the vehicle inertial dynamics in roll, pitch and yaw motions when it is subjected to longitudinal, lateral and vertical forces. Compliance characteristics in vehicle suspension systems are usually of a non-linear nature.

Vehicle handling analysis, through multi-body dynamics, received an impetus with the work of McHenry [**2**]. A considerable volume of literature deals with the issue of ride comfort of vehicles in single-event perturbations such as negotiating a bump or a ditch. Other analyses are concerned with vehicle handling characteristics in response to various intended manoeuvres. The performance characteristics of a vehicle in all such tests are profoundly affected by its suspension, a primary function of which is ride comfort. Another function of the suspension system is to maintain the road wheels at correct orientations to the road surface, and thus control the directional response of the vehicle during the various manoeuvres. Often, for good ride comfort the suspension system should provide a relatively low vertical stiffness, which conflicts with the requirements of good handling analysis which usually calls for a relatively high value of stiffness. These conflicting requirements have led to the gradual introduction of independent suspensions, adjustable systems and active elements. Suspensions may also be designed so that the stiffness of the bushes contributes to the overall roll stiffness of the vehicle.

Chace [**3**] and Orlandea *et al*. [**4, 5**] have investigated a three-dimensional vehicle model with 42 rigid-body degrees of freedom. They subjected their model to a severe steering ramp input of 210° in 0.4 s while travelling at a forward tangential speed of 75 km/h. The simulation results were presented for lateral acceleration, roll angle and yaw velocity. Allen *et al*. [**6**] reported two vehicle models: a linear and a non-linear dynamic model. They also proposed a numerical procedure designed to permit efficient vehicle dynamic analysis on a microcomputer of the type in use at that time. Their analyses include a steady state model for the determination of side force coefficients, a stability factor and time of manoeuvre for lateral/directional control. The steady state and dynamic models included a tyre model for comprehensive slip. Pacejka [**7**] introduced handling diagrams for the analysis of the steady state behaviour of a vehicle. A handling diagram was defined as the plot of lateral acceleration versus the difference between the slip angles of rear and front tyres. Naude and Steyn [**8**] have investigated a computer simulation for the handling characteristics of a vehicle, performing a double-lane change manoeuvre in order to perform a transient handling simulation. They have also presented a driver model to steer the vehicle along a prescribed path during their closed-loop simulation study.

In order to study the handling behaviour of a vehicle, the tyre cornering forces must be carefully determined. The simplest form of tyre modelling involves the computer storage of a large amount of measured tyre data which are used in conjunction with an interpolation method to represent the tyre forces characterized by the measured data. This method is currently used in general purpose dynamics software. Most tyre models currently used in vehicle dynamic simulations involve empirical representations of the measured tyre data. A comprehensive review of the tyre models is given by Pacejka and Sharp [**9**].

Pacejka *et al*. [**10**] employed a tyre formula to describe the characteristics of side force and self-aligning torque as functions of slip angle, and the longitudinal force (brake force) as a function of longitudinal slip, with good accuracy. The formula is limited to steady state conditions during pure cornering and pure braking. This tyre model contains 53 coefficients, which define the tyre stiffness components, tyre geometry and peak force variations with slip angle or longitudinal slip. The formula also takes into account the curvature factors, which are functions of vertical load and camber angle. The model has come to be known as the 'magic formula', representing an empirical method for fitting tyre data.

Allen *et al*. [**11, 12**] investigated an expanded version of vehicle simulation tyre models for a full range of operating conditions (slip, camber and normal load) on both paved and off-road surfaces. Their tyre model simulations are based upon a composite slip formulation as a function of lateral and longitudinal slip. Xia and Willis [**13**] have studied the effect of tyre cornering stiffness on the vehicle frequency response, using two different models. These include a non-linear vehicle model and a linear bicycle model that has two degrees of freedom. The non-linear vehicle model employs a multi-body dynamics formulation and includes a non-linear steering system, full suspension geometry, non-linear suspension forces and the non-linear tyre forces and moments. The linear model was considered as a linear time-invariant system with two degrees of freedom and included the evaluation of lateral velocity and yaw rate of the vehicle with constant forward speed.

In fact, vehicle ride and handling analysis has accounted for one of the largest growth areas in the application of multi-body dynamics. Various literature reviews are provided by Kortüm and Sharp [**14**], Kortüm and Schiehlen [**15**] and Kübler and Schiehlen [**16**].

2 DESCRIPTION OF THE VEHICLE MODEL

The full vehicle model comprises vehicle mass and inertia, front and rear double-wishbone suspensions, a rack and pinion steering system, road wheels and tyres. Vehicle motions are described in terms of the fixed global frame of

K00199 © IMechE 1999

reference X, Y, Z shown in Fig. 1. Local part frames of reference x_i, y_i, z_i are attached to all of the moving parts i. A generic formulation method, based upon Lagrange's equation for constrained systems, is employed for the derivation of equations of motion for all parts in the model in a body 3–1–3 Euler frame of reference (see Section 3).

2.1 Suspensions and steering system models

The front and rear suspensions are of double-wishbone configuration. Each quarter-suspension comprises two control arms, referred to as the lower and upper control arms respectively. The control arms are connected to the vehicle body by elastic rubber bushings with non-linear characteristics. Typical characteristic curves for these are shown in Fig. 2. The bushings provide appropriate longitudinal and torsional compliance which influences the dive (during braking) and squat (during acceleration) characteristics of the vehicle. The shock absorber is attached to the vehicle underbody and the lower control arm. A bump stop is situated on the lower control arm, while a rebound stop is located on the upper control arm. Typical characteristics for these elements are also shown in Fig. 2.

The upper steering column is connected to the steering wheel and to the vehicle body by revolute joints, and to the lower steering column by a universal joint (see Fig. 3). The pinion is connected to the steering column by a universal joint, and to the vehicle body by a cylindrical joint. The steering rack is connected to the vehicle body by a translational joint. The coupler connects between the cylindrical and translational joints, describing their motion relationship which is 166 mm of rack travel resulting from 1148.4° of pinion rotation. The steering rack is connected to the tie rods by universal joints. The tie rods are attached to the steering knuckles by spherical joints which represent the ball joints, also shown in Fig. 3. The steering knuckles, in turn, are connected to the upper and lower control arms by spherical joints in appropriate locations which define the inclination of the steering axis.

2.2 Tyre model

There are six components of force and moment generated as a result of tyre interaction with the road. These are the vertical tyre force, longitudinal traction force and lateral force, as well as the self-aligning moment, the overturning moment and the rolling resistance moment (see Fig. 4a). The tyre model reported here does not include the overturning moment.

2.2.1 Tyre vertical force

The radial tyre contact force, acting in the radial plane of the tyre, has a component that acts in the direction of the contact normal at the tyre–road contact patch. This component is used to calculate the tyre vertical force. The radial force is dependent on tyre deflection and its rate of change, both measured along the tyre vertical directional vector [**17**]. The deflection is obtained by an instantaneous evaluation of the distance between the position of the wheel centre and the road surface plane in the contact patch. The time rate of change in deflection is obtained by the vector scalar product of the instantaneous tyre radius vector and the wheel centre global velocity. The quantities thus obtained are employed to obtain the stiffness and damping contributions to the tyre vertical force, as indicated by the first and second terms in equation (1):

$$F_{\text{vert}} = k\delta - c\frac{\partial \delta}{\partial t} \tag{1}$$

2.2.2 Tyre lateral force

There are two alternative methods for determination of the tyre lateral force. These are through the use of an equation

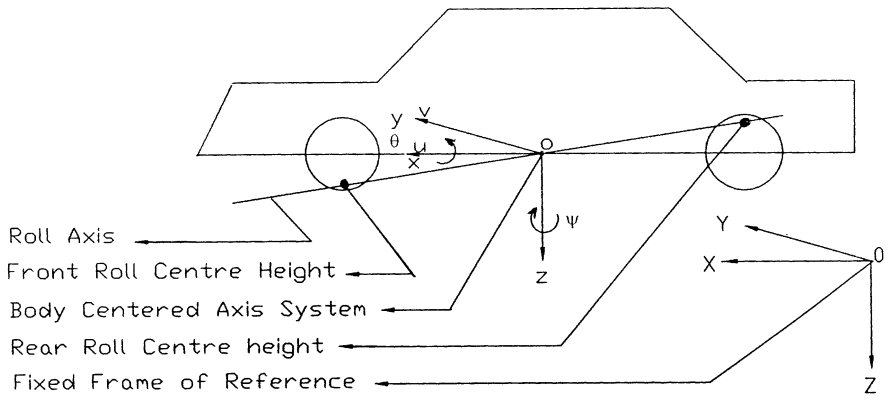

Fig. 1 Axis system for the vehicle model

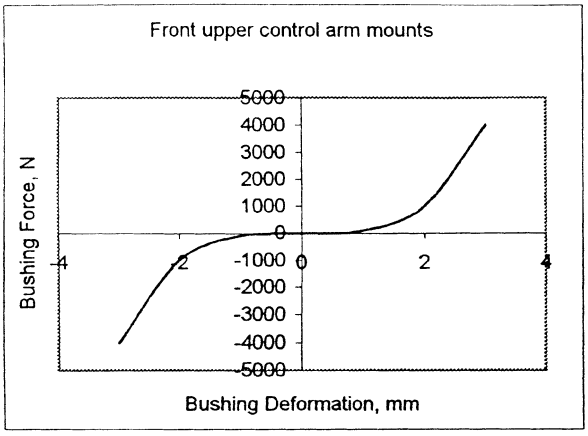

(a) Sub-frame mounts

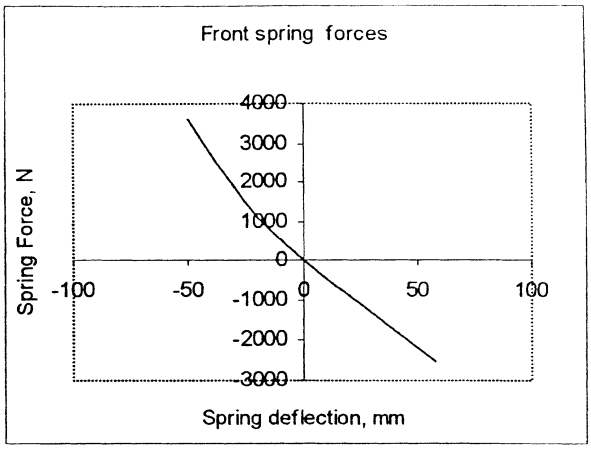

(b) Front spring characteristics

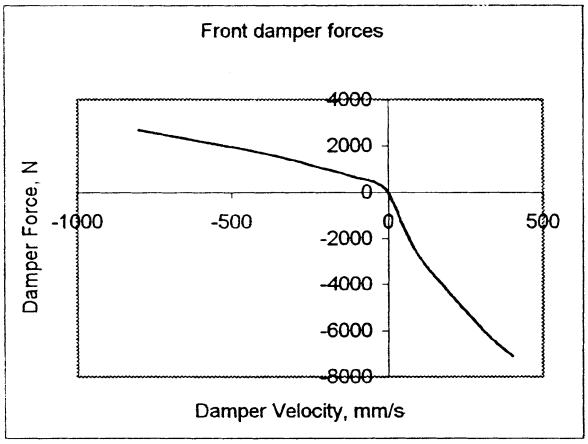

(c) Front damper characteristics

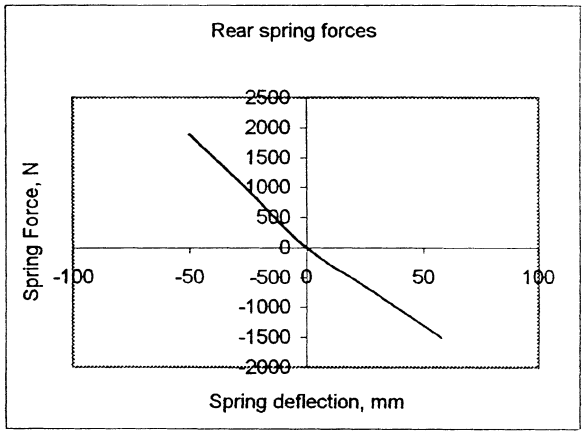

(d) Rear spring characteristics

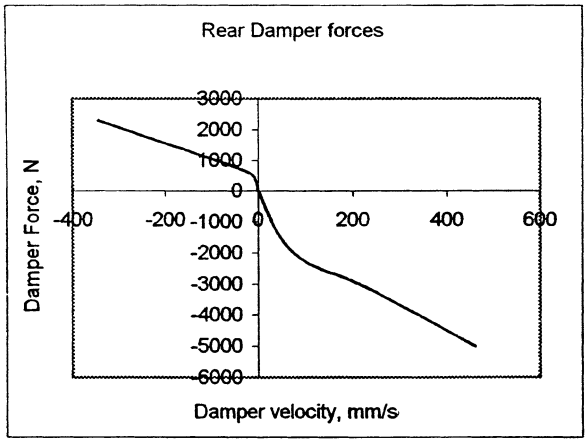

(e) Rear damper characteristics

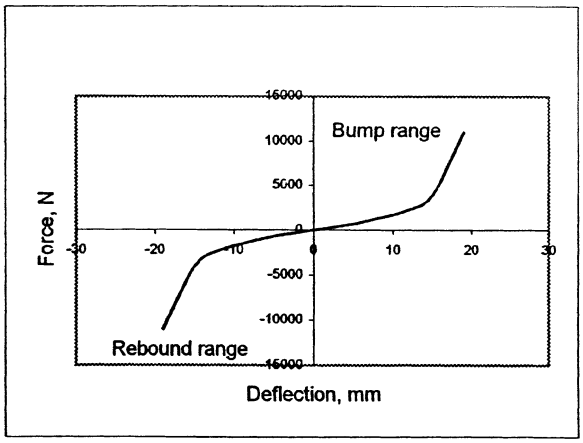

(f) Bump and Rebound stop force characteristics

Fig. 2 Sources of compliance in the vehicle model

Parts

3	Steering rack
4	Steering wheel
5	Upper steering col.
6	Lower steering col.
7	Pinion
8	Lower wishbone left
9	Lower wishbone right
10	Upper wishbone left
11	Upper wishbone right
12	Steering knuckle left
13	Steering knuckle right
14	Tie rod left
15	Tie rod right
16	Upper damper left
17	Upper damper right
18	Lower damper left
19	Lower damper right
32	Front tyre left
33	Front tyre right

Joints

1	Revolute joint /26
2	Revolute joint /33
3	Universal joint
4	Universal joint
5	Cylindrical joint /54
6	Translational joint /61
7	Spherical joint
8	Spherical joint
9	Spherical joint
10	Spherical joint
11	Spherical joint
12	Spherical joint
13	Universal joint
14	Universal joint
15	Cylindrical joint
16	Cylindrical joint
25	Revolute joint
26	Revolute joint
29	Coupler
30	Motion
31	Motion

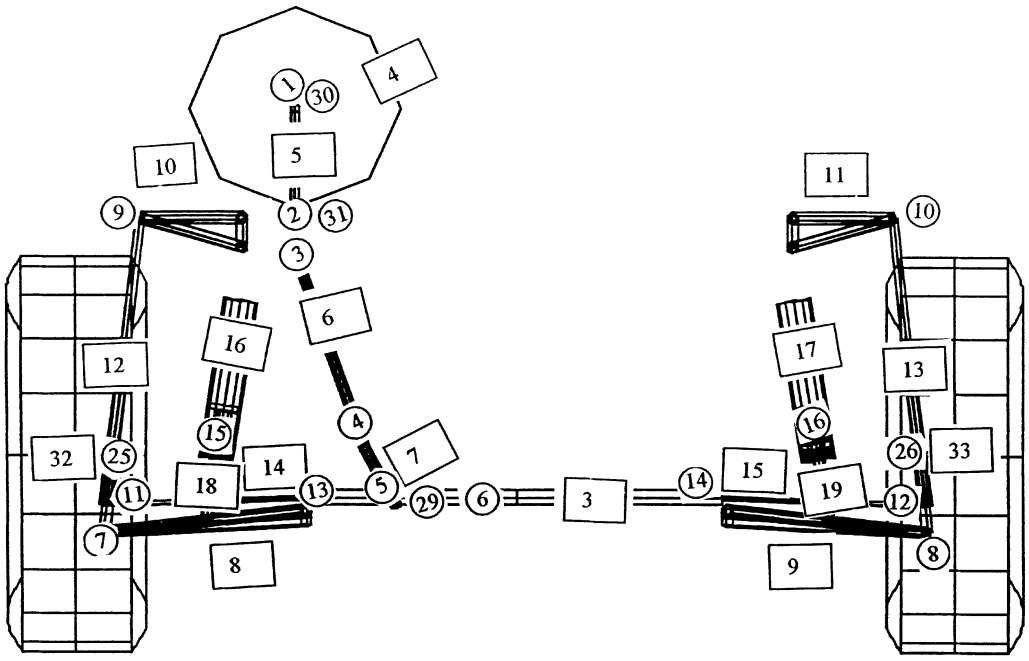

Fig. 3 Schematic representation of front vehicle suspension and steering system

method or by an interpolation process [**17**]. The equation method, employed in this analysis uses the following simplified equation to generate the lateral force:

$$F_{\text{lat}} = \mu F_{\text{vert}}(1 - \mathrm{e}^{-k_{\text{lat}}|\alpha|}) \tag{2}$$

where

$$\alpha = \tan^{-1}\left(\frac{v + l\psi_{10}}{u}\right) - \beta \tag{3}$$

For $\alpha = \alpha_{\text{f}}$, $l = a$ and $\alpha = \alpha_{\text{r}}$, $l = -b$. The coefficient of friction μ changes from the initial static to the instantaneous dynamic conditions as shown in Fig. 4b.

2.2.3 *Tyre longitudinal force*

The rolling resistance force and the traction (or braking) force together constitute the tyre longitudinal reaction force [**17**]. The rolling resistance force is calculated by multiplying the coefficient of rolling resistance, f, with the vertical force. The traction force is obtained by multiplying the instantaneous value of the coefficient of friction with the vertical force. These forces oppose the motion of the

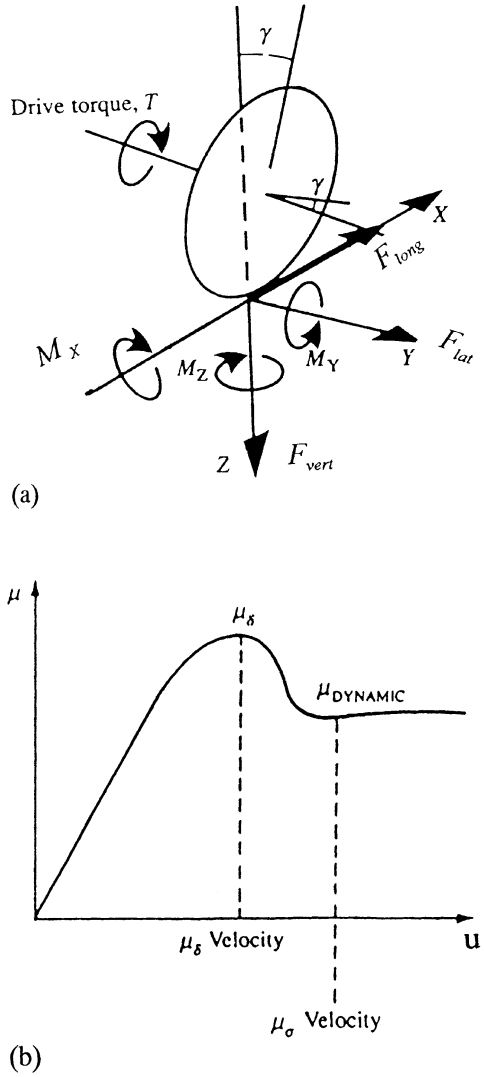

Fig. 4 (a) Tyre forces and moments and (b) variation in coefficient of friction with longitudinal speed

vehicle at the road surface contact patch. The combined force is referred to as the longitudinal force:

$$F_{\text{long}} = (\mu - f)F_{\text{vert}} \tag{4}$$

2.3 Vehicle model

The full vehicle model is an assembly of the front suspension and steering system, the rear suspension, the road wheels and tyres. It also includes the vehicle body, represented by its mass and inertial components. Tables 1 and 2 provide the list of all parts and all constraints in the full vehicle model.

The Grüebler–Kützbach expression can be used to determine the available degrees of freedom in the vehicle model. There are 34 parts in the vehicle model, excluding ground (see Table 1). The number of constraints for each joint, coupler and specified motions is given in Table 2. Thus:

$$n_{\text{DOF}} = 6n - \sum \text{constraints} = 6n - m = 6(34) - 110$$

$$= 94 \tag{5}$$

3 METHOD OF FORMULATION AND SOLUTION

3.1 Equations of motion

There are 34 parts in the multi-body model, the motion of each of which can be described in terms of the generalized coordinates, q, by Lagrange's equation for constrained systems:

$$\frac{\mathrm{d}}{\mathrm{d}t}\left(\frac{\partial K}{\partial \dot{q}}\right) - \frac{\partial K}{\partial q} - F_q + \sum_{k=1}^{m} \lambda_k \frac{\partial C_k}{\partial q} = 0 \tag{6}$$

The generalized coordinates are given by $\{q\}^{\mathrm{T}} = \{x\ y\ z\ \psi\ \theta\ \varphi\}$, where the rotational components are the Euler angles in body 3–1–3 successive rotations.

The reaction forces in the multibody system are given by the summation term in equation (6) along each of the generalized coordinates. These are introduced as holonomic algebraic constraint functions, C_k. Therefore, the assembly of parts can be represented mathematically in a manner that conforms to the required dynamic functions of the system. Under dynamic conditions, equation (6) provides six equations of motion per part in the vehicle system model.

3.2 Holonomic constraint functions

Ideal functions in all mechanisms are assured by appropriate use of constraints in the form of joints or attachments. Each joint or assembly attachment introduces constraint functions in the form of non-linear algebraic equations. Table 2 lists the different types of joint employed in the assembly of various parts in the vehicle model. Typical constraint functions for a number of these joints are given below.

For a spherical joint, for instance between the steering left front knuckle and its upper wishbone, the following three constraints pertaining to an at-point condition exist:

$$C_{k=1-3} = x_{22,24} = y_{22,24} = z_{22,24} = 0 \tag{7}$$

For a revolute joint, as in the attachment between the upper steering column and the steering wheel, the at-point constraint is supplemented by two-axis orthogonality conditions around the rotation $\psi_{5,4}$:

$$C_{k=1-3} = x_{5,4} = y_{5,4} = z_{5,4} = 0 \tag{8}$$

K00199 © IMechE 1999

Table 1 Mass and inertial properties in the vehicle model

			Centre of mass location (mm)			Inertia (kg/mm^2)		
No.	Part name	Mass (kg)	X	Y	Z	I_{xx}	I_{yy}	I_{zz}
1	Ground	—	—	—	—	—	—	—
2	Vehicle body	1185	1200	0	160	4.83E+08	2.404E+09	2.482E+09
3	Steering rack	4.1	−697	0	−128.8	1.84E+05	1.84E+05	460
4	Steering wheel	2.1	674	396	574	1.3E+04	1.3E+04	2.4E+04
5	Upper steering column	1.6	295.5	396	450.5	8.5E+04	8.5E+04	80
6	Lower steering column	1.1	−355.5	333.5	138.5	3.4E+04	3.4E+04	40
7	Pinion	0.8	−639	243.5	−92	3200	3200	77
8	Lower wishbone left	6	−447	−489.3	−166.6	5E+04	1E+05	1.5E+05
9	Lower wishbone right	6	−447	489.3	−166	5E+04	1E+05	1.5E+05
10	Upper wishbone left	0.6	−553	−556.4	373	3000	300	3000
11	Upper wishbone right	0.6	−553	556.4	373	3000	300	3000
12	Steering knuckle left	14	−516.3	−767.4	−39.5	8E+04	1.3E+05	8E+04
13	Steering knuckle right	14	−516.3	767.4	−39.5	8E+04	1.3E+05	8E+04
14	Tie rod left	0.7	−701.3	−549	−134.9	8200	8200	27
15	Tie rod right	0.7	−701.3	549	−134.9	8200	8200	27
16	Upper damper left	15.12	−572.9	−507.3	128.1	1.4E+05	1.4E+05	2.7E+04
17	Upper damper right	15.12	−572.9	507.3	128.1	1.4E+05	1.4E+05	2.7E+04
18	Lower damper left	1.68	−574.9	−538.8	−74.2	6000	6000	200
19	Lower damper right	1.68	−574.9	538.8	−74.2	6000	6000	200
20	Lower wishbone left	1.8	2526	−522	−177	1.5E+04	1E+05	2.4E+04
21	Lower wishbone right	1.8	2526	522	−177	1.5E+04	1E+05	2.4E+05
22	Upper wishbone left	1.3	2513	−579.5	92.6	7000	1.5E+04	2.1E+04
23	Upper wishbone right	1.3	2513	579.5	92.6	7000	1.5E+04	2.1E+04
24	Steering knuckle left	13.8	2520	−764	−39	8.2E+04	1.31E+05	8.2E+04
25	Steering knuckle right	13.8	2520	764	−39	8.2E+04	1.31E+05	8.2E+04
26	Tie rod left	0.7	2700.4	−555.1	−141.8	8200	8200	27
27	Tie rod right	0.7	2700.4	555.1	−141.8	8200	8200	27
28	Upper damper left	15.12	2478.6	−543.7	109.4	1.4E+05	1.4E+05	2.7E+04
29	Upper damper right	15.12	2478.6	543.7	109.4	1.4E+05	1.4E+05	2.7E+04
30	Lower damper left	1.68	2469.6	−559.8	−95.4	6000	6000	200
31	Lower damper right	1.68	2469.6	559.8	−95.4	6000	6000	200
32	Front tyre left	42.2	−573	−767.1	−51	9E+05	9E+05	1.59E+06
33	Front tyre right	42.2	−573	767.1	−51	9E+05	9E+05	1.59E+06
34	Rear tyre left	42.2	2577	−756	−51	9E+05	9E+05	1.59E+06
35	Rear tyre right	42.2	2577	756	−51	9E+05	9E+05	1.59E+06

and

$$C_{k=4} = \sin\theta_{5,4}\sin\phi_{5,4} = 0 \quad \text{and}$$

$$C_{k=5} = \sin\theta_{5,4}\cos\phi_{5,4} = 0 \tag{9}$$

A cylindrical joint, for instance between the pinion gear and the vehicle body, with the degrees of freedom $z_{7,10}$, $\psi_{7,10}$, has the following constraint functions:

$$C_{k=1} = x_{7,10}(\sin\psi_{7,10}\cos\theta_{7,10}\sin\phi_{7,10} - \cos\psi_{7,10}\cos\phi_{7,10}) = 0 \tag{10}$$

$$C_{k=2} = y_{7,10}(\cos\psi_{7,10}\cos\theta_{7,10}\cos\phi_{7,10} - \sin\psi_{7,10}\sin\phi_{7,10}) = 0 \tag{11}$$

$$C_{k=3} = \sin\theta_{7,10}\sin\phi_{7,10} = 0 \tag{12}$$

$$C_{k=4} = \sin\theta_{7,10}\cos\phi_{7,10} = 0 \tag{13}$$

The $z_{3,10}$ translational motion of the steering rack with respect to the vehicle body has the constraint functions

$$C_{k=1} = x_{3,10}(\sin\psi_{3,10}\cos\theta_{3,10}\sin\phi_{3,10} - \cos\psi_{3,10}\cos\phi_{3,10}) = 0 \tag{14}$$

$$C_{k=2} = y_{3,10}(\cos\psi_{3,10}\cos\theta_{3,10}\cos\phi_{3,10} - \sin\psi_{3,10}\sin\phi_{3,10}) = 0 \tag{15}$$

$$C_{k=3} = \sin\psi_{3,10}\cos\phi_{3,10} + \cos\psi_{3,10}\cos\theta_{3,10}\sin\phi_{3,10} = 0 \tag{16}$$

$$C_{k=4} = -\cos\psi_{3,10}\sin\theta_{3,10} = 0 \tag{17}$$

$$C_{k=5} = \sin\psi_{3,10}\sin\theta_{3,10} = 0 \tag{18}$$

The steering motion for the vehicle manoeuvre is given as a function of time (see Fig. 5). This presents a single constraint function as

Table 2 Assembly constraints in the vehicle model

No.	Constraint type	Part I	Part J	Joint location (mm)			No. of constraints
				X	*Y*	*Z*	
1	Revolute joint/26	Steering wheel	Upper steering column	674	396	574	5
2	Revolute joint/33	Upper steering column	Vehicle body	295.5	396	450.5	5
3	Universal joint	Upper steering column	Lower steering column	−114	396	317	4
4	Universal joint	Lower steering column	Pinion	−597	271	−40	4
5	Cylindrical joint/54	Pinion	Vehicle body	−639	234.5	−92	4
6	Translational joint/61	Steering rack	Vehicle body	−697.5	0	−128.8	5
7	Spherical joint	Lower wishbone left	Steering knuckle left	−580.3	−731.9	−191.4	3
8	Spherical joint	Lower wishbone right	Steering knuckle right	−580.3	731.9	−191.4	3
9	Spherical joint	Upper wishbone left	Steering knuckle left	−550.8	−670.4	376.6	3
10	Spherical joint	Upper wishbone right	Steering knuckle right	−550.8	670.4	376.6	3
11	Spherical joint	Steering knuckle left	Tie rod left	−705.1	−730.9	−140.9	3
12	Spherical joint	Steering knuckle right	Tie rod right	−705.1	730.9	−140.9	3
13	Universal joint	Steering rack	Tie rod left	−697.5	−367	−128.8	4
14	Universal joint	Steering rack	Tie rod right	−697.5	367	−128.8	4
15	Cylindrical joint	Upper damper left	Lower damper left	−574.5	−531.9	−29.8	4
16	Cylindrical joint	Upper damper right	Lower damper right	−574.5	531.9	−29.8	4
17	Spherical joint	Lower wishbone left	Steering knuckle left	2569.7	−743.4	−192	3
18	Spherical joint	Lower wishbone right	Steering knuckle right	2569.7	743.4	−192	3
19	Spherical joint	Upper wishbone left	Steering knuckle left	2584.9	−705.9	100	3
20	Spherical joint	Lower wishbone right	Steering knuckle right	2584.9	705.9	100	3
21	Spherical joint	Steering knuckle left	Tie rod left	2704.2	−742.4	−148.7	3
22	Spherical joint	Steering knuckle right	Tie rod right	2704.2	742.4	−148.7	3
23	Cylindrical joint	Upper damper left	Lower damper left	2471.6	−556.2	−49.9	4
24	Cylindrical joint	Upper damper right	Lower damper right	2471.6	556.2	−49.9	4
25	Revolute joint	Steering knuckle left	Front tyre left	−573	−780.8	−51	5
26	Revolute joint	Steering knuckle right	Front tyre right	−573	780.8	−51	5
27	Revolute joint	Steering knuckle left	Rear tyre left	2577	−756	−51	5
28	Revolute joint	Steering knuckle right	Rear tyre right	2577	−756	−51	5
29	Coupler	Joint 54	Joint 61				1
30	Motion		Joint 26				1
31	Motion		Joint 33				1

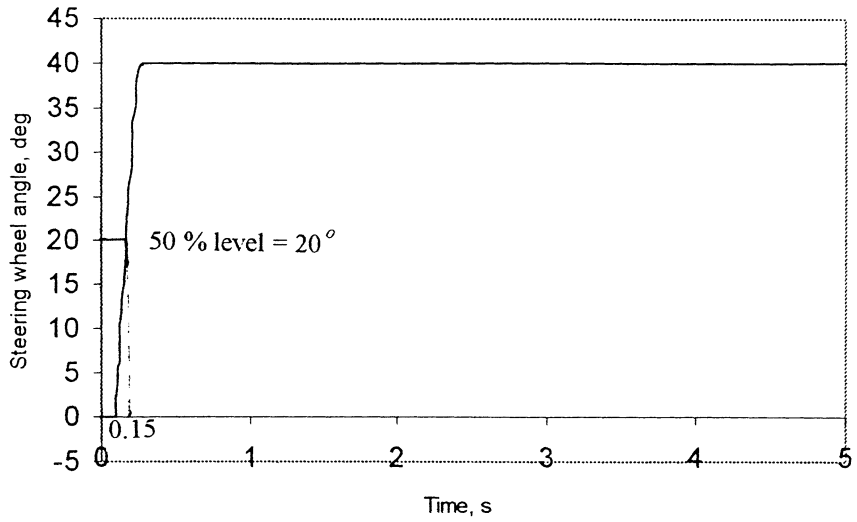

Fig. 5 Steering wheel angle input with time

$$\beta = \begin{cases} 0, & t \leqslant 0.1 \\ 0.11\pi\left\{1 + \sin\left[\dfrac{\pi(t-0.1)}{0.2} - \dfrac{\pi}{2}\right]\right\}, & 0.1 \leqslant t \leqslant 0.3 \\ 0.22\pi, & t \geqslant 0.3 \end{cases} \tag{19}$$

There are, in fact, 110 constraint functions in the vehicle model, similar to constraint functions (8) to (19).

3.3 Formation of the Jacobian matrix

The set of differential equations of motion (Section 3.1), the scalar constraint functions (Section 3.2), the applied forces

and the compliance functions (e.g. tyre forces, bushing reactions) have to be solved in discrete small time steps. The vector of unknowns includes the system state variables (position, velocity and acceleration of all parts) and the Lagrange multipliers representing the joint reactions. Thus, in matrix form the set of equations is represented by

$$[\mathbf{J}]\{\boldsymbol{q},\ \lambda\}^{\mathrm{T}} = \{\boldsymbol{F}_q\} \tag{20}$$

The Jacobian matrix is of the following form:

$$[\mathbf{J}] = \begin{bmatrix} \left[\dfrac{s}{\mathrm{d}t}\dfrac{\partial K}{\partial q} + \dfrac{\partial K}{\partial q}\right] & \left[\dfrac{\partial C}{\partial \lambda}\right] \\ \left[\dfrac{\partial C}{\partial q}\right] & [0] \end{bmatrix} \tag{21}$$

The Jacobian matrix contains many zero entries, thus being referred to as sparse. The Jacobian matrix is also quite large in dimensions, as it embodies appropriate coefficients for six equations of motion for all the vehicle parts listed in Table 1, and all the formulated constraint functions for the joints in the model (see Table 2 and Section 3.2). In fact fewer than 10 per cent of all the elements of the matrix are usually non-zero. The solution to the differential-algebraic set of equations is obtained in small variable time steps, dt, employing a predictor–corrector technique with a Newton–Raphson method for the solution of a non-linear set of simultaneous equations, and step-by-step integration using a 'stiff' algorithm for widely split eigenvalue problems [**18–20**].

4 FULL-VEHICLE SIMULATION STUDIES AND DISCUSSION

An important measure of vehicle performance is its handling characteristics when subjected to a given steering input. The stability of the vehicle under various specified manoeuvres can be investigated. Typical vehicle handling simulations include transient cornering, lane changing and slalom motions, including double-lane changes, with or without braking. The current analysis is concerned with a transient cornering manoeuvre with a constant forward velocity. A number of important parameters are investigated. These include the tyre forces, spring forces, damper forces and bump and rebound stop forces, particularly on the inside wheels as the vertical force diminishes with increasing lateral acceleration. The vertical excursion of the front and rear roll centre heights is also of interest as a large displacement of these can affect the vehicle stability.

Most modern vehicles can undergo cornering manoeuvres with lateral accelerations of up to 0.8 g, during which body roll in the region 2–8° can occur. The specified manoeuvre should represent a realistic test of vehicle behaviour under severe conditions. Test procedures have been specified by international standards in ISO 7401–1988 or in the British Standard BS AU 230:1989 [**21**].

Figure 6 shows an animated output for the transient manoeuvre during a simulation time of 5 s. Five hundred time steps of simulation were undertaken, after an initial static equilibrium analysis is carried out to ensure vehicle placement at the kerb height.

Figures 7a and b show the vertical tyre forces during the specified manoeuvre. The tyre forces at time $t = 0$ correspond to the initial static equilibrium position. Due to the weight distribution of the vehicle, the rear tyres carry approximately 54.5 per cent of the total weight. The corresponding front and rear roll centre heights are 70.3 and 76.7 mm above the ground respectively. During the manoeuvre, as the steering wheel input increases from 0 to 40°, the outside wheels generate larger vertical tyre forces owing to the inertial forces, which effect a load transfer

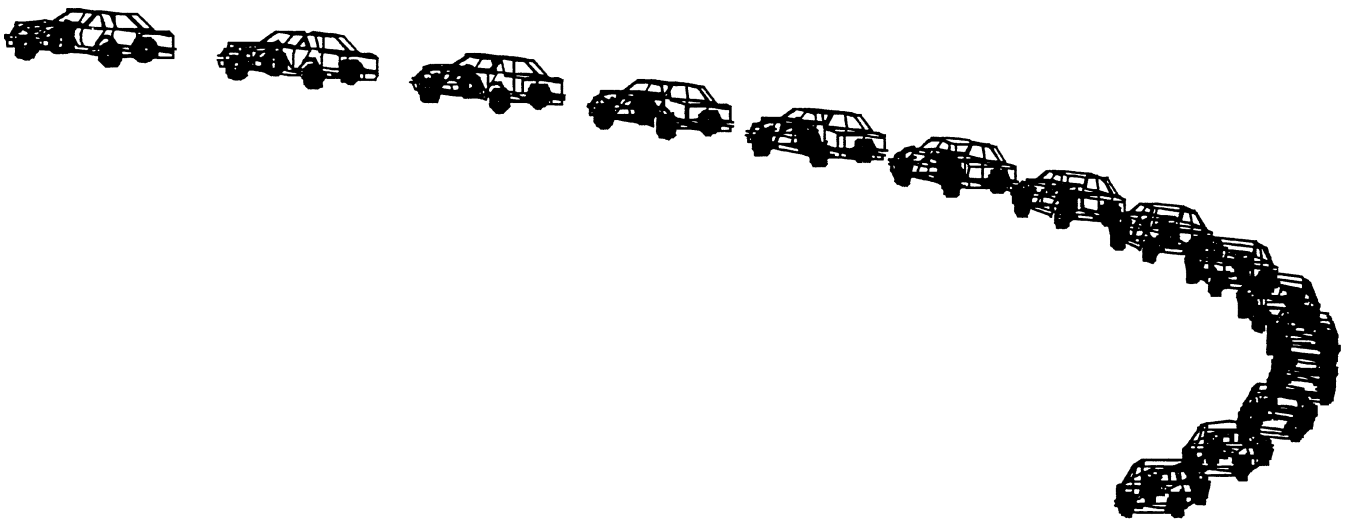

Fig. 6 Vehicle manoeuvre for 5 s of simulations

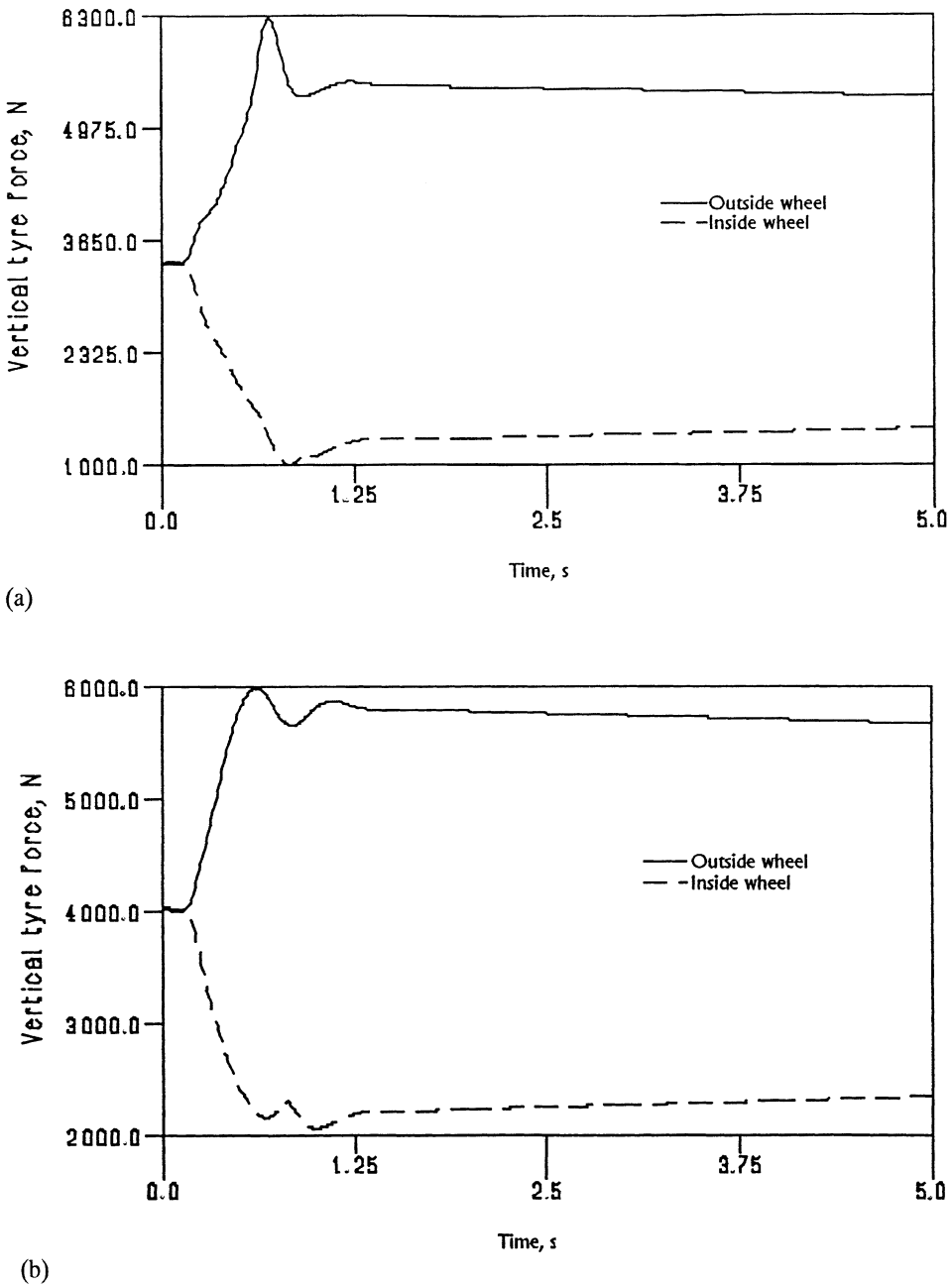

Fig. 7 Vertical forces for (a) front tyres and (b) rear tyres

from right to left. Therefore, the vertical tyre forces on the outside wheels increase and generate a bump stop force in the opposite direction. Consequently, the vertical tyre forces on these wheels decrease. The inside wheels are subjected to the opposite effect owing to rebound. This trend can be observed in Figs 7a and b. The bump and rebound forces are shown in Figs 8a and b, corroborating this argument. The reduction in the vertical tyre force on the inside wheels is an indication of vehicle instability. It can be observed that for this simulation the inside wheels off-load rapidly before a steady condition is reached through body roll, suspension articulation and generation of shock absorber reactions. The inside wheel tyres still carry sufficient vertical forces to maintain a good contact with the road. It should also be noted that the transient response dies down quickly after a few oscillations, this being an indication of an acceptable response of the vehicle to the steering input. The front and rear roll centres undergo vertical excursions towards the ground with downward articulation of the control arms (see Fig. 9a).

Reference [**21**] outlines the standard test for the transient response of a vehicle subjected to a step input steering

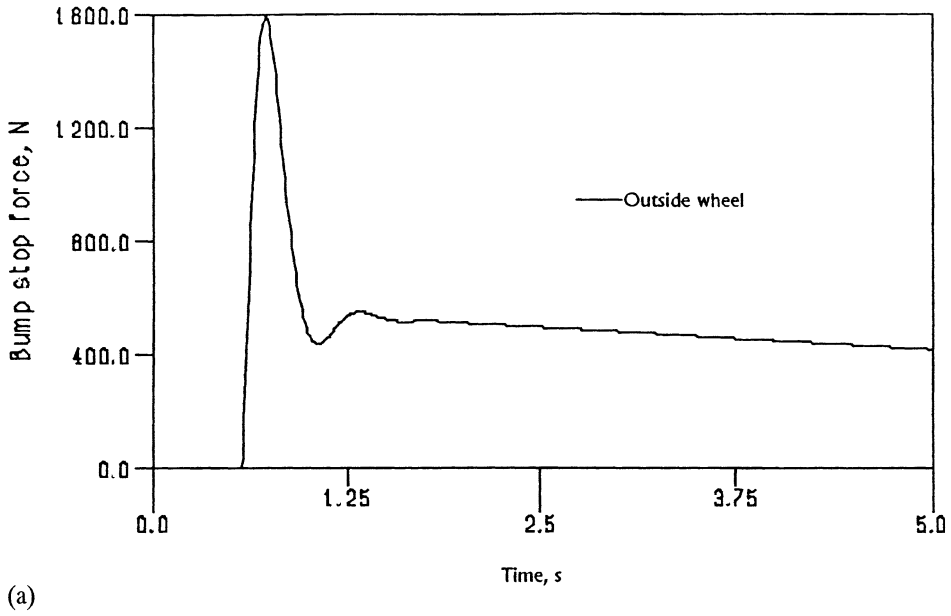

(a)

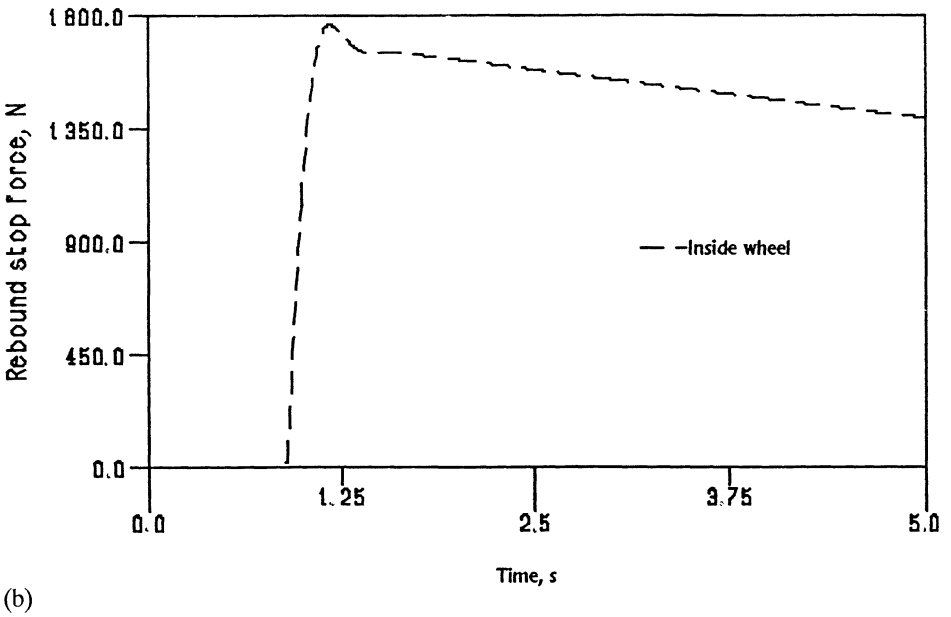

(b)

Fig. 8 (a) Bump stop forces for front tyres and (b) rebound stop forces for front tyres

function. Under this test, the variations in the response (i.e. roll angle, lateral acceleration and yaw rate) can be obtained as measures of vehicle performance. Figures 9b and c illustrate the lateral acceleration and roll angle change for the step steering input shown in Fig. 5 and equation (19). Both the lateral acceleration and the roll angle rise with an increasing steering angle. The maximum steering angle is 40°, reached after 0.3 s. In this standard transient response test the vehicle response time is defined as the period taken for the vehicle to reach 90 per cent of the maximum response value, if the origin of the time base is set at the point where half the maximum steering input has been accomplished. The response time for the lateral acceleration is, therefore, 0.39 s (see Fig. 9b). The peak response time is also measured in the same time frame. This is also shown in the same figure and is 0.56 s. The parameters of interest in this transient analysis are the response time, the peak response time and the lateral acceleration overshoot. Clearly, optimal conditions relate to the minimization of all of these parameters. The same parameters can also be measured from the variation in roll angle in Fig. 9c. These are shown in the figure.

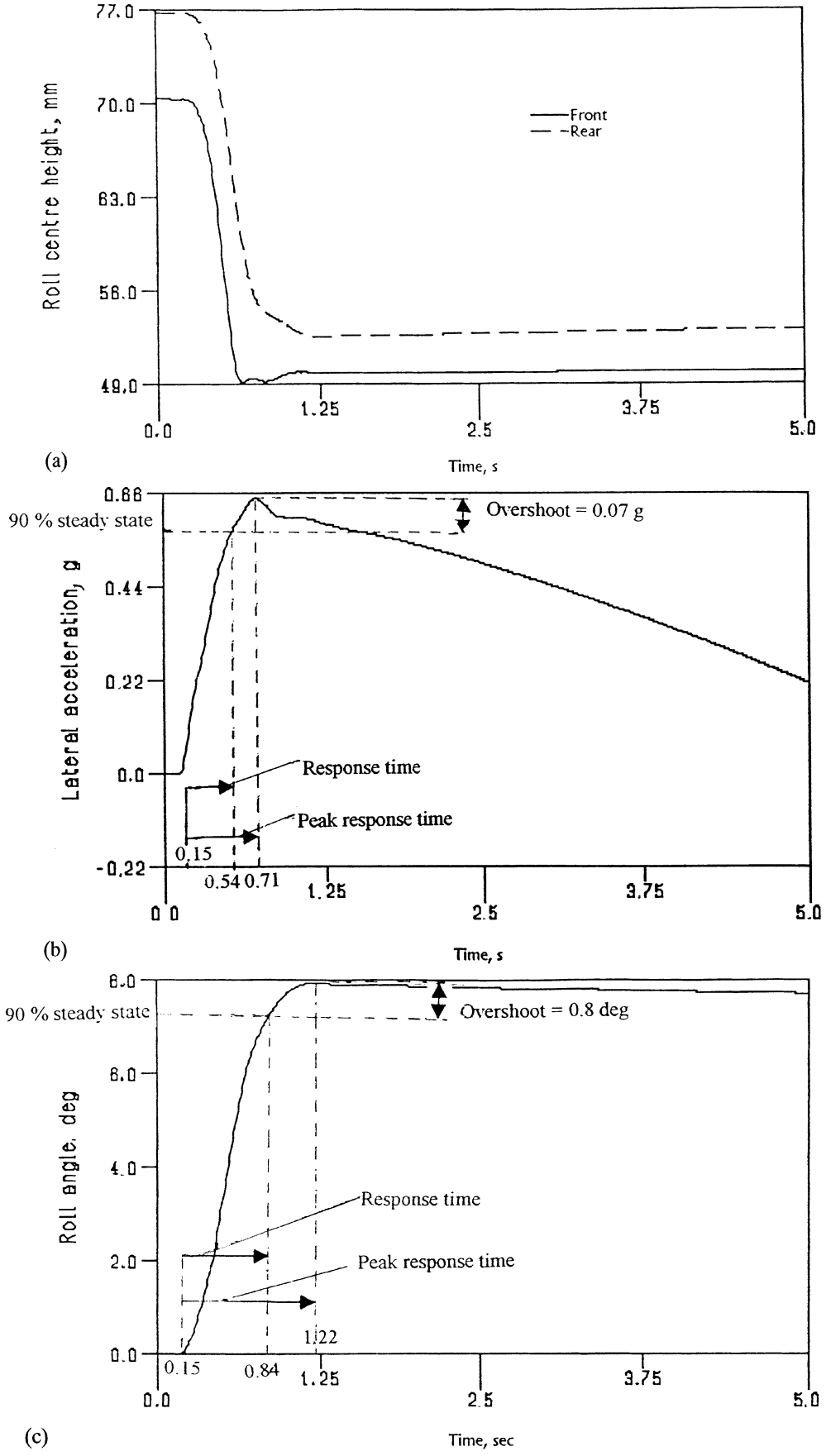

Fig. 9 (a) Instantaneous roll centre height variation, (b) lateral acceleration variation with time and (c) vehicle body roll angle variation with time

5 CONCLUSION

This paper has shown the use of multi-body dynamics in vehicle handling analysis. This approach is particularly useful under transient conditions arising from the application of a steering function. A non-linear dynamic analysis for a realistic multi-degrees-of-freedom vehicle model (having 94 degrees of freedom) subjected to a step steering function has been presented. The results of such an analysis can be used to measure the vehicle 'responsiveness' in terms of given parameters specified in ISO and BS standards for non-steady conditions. The extent of lateral acceleration overshoot, roll angle variation and generated vertical tyre forces, particularly on the inside wheels, in turn can provide a good measure of vehicle stability. The simulation highlighted in the paper indicates that sufficient tyre forces are generated, ensuring vehicle adherence to its path. The change in the roll angle is within the specified limit for the type of vehicle under investigation. The vehicle lateral acceleration overshoot is $0.07\,g$ and its response time to the steering input is adequately short. The procedure highlighted in this paper can be employed for simulation of vehicle models under transient manoeuvres. A large amount of proprietary physical and geometrical data has been included in the paper which can be used by others who intend to carry out similar vehicle handling studies.

ACKNOWLEDGEMENT

The authors wish to express their gratitude to the Egyptian Military Attaché's Office for the financial support extended to this research project.

REFERENCES

1 **Segel, L.** Theoretical prediction and experimental substantiation of the response of the automobile to steering control, in research in automobile stability and control and in tyre performance. *Proc. Instn Mech. Engrs*, 1956–7, (7), 310–330.
2 **McHenry, R. R.** An analysis of the dynamics of automobiles during simultaneous cornering and ride motions, in handling of vehicles under emergency conditions. *Proc. Instn Mech. Engrs*, 1968–9, (13), 28–48.
3 **Chace, M. A.** Methods and experience in computer aided design of large displacement mechanical systems. *Computer Aided Analysis and Optimization of Mechanical System Dynamics*, Nato ASI Series, F9, 1984, pp. 233–259.
4 **Orlandea, N., Chace, M. A.** and **Calahan, D. A.** A sparsity-oriented approach to the dynamic analysis and design of mechanical systems, Parts I and II. *Trans. ASME, J. Engng for Industry*, 1977, **99**, 773–784.
5 **Orlandea, N.** and **Chace, M. A.** Simulation of a vehicle suspension with ADAMS computer program. SAE Technical paper 770053, 1977.
6 **Allen, R. W., Rosenthal, T. J.** and **Szostak, T. H.** Steady state and transient analysis of ground vehicle handling. SAE Technical paper 870495, 1987, pp. 49–78.
7 **Pacejka, H. B.** Simplified analysis of steady state turning behaviour of motor vehicle—Part 1: handling diagram of simple system. *Veh. Syst. Dynamics*, 1973, **2**, 161–172.
8 **Naude, A. F.** and **Steyn, J. L.** Objective evaluation of the simulated handling characteristics. SAE Technical paper 930826, 1993, pp. 97–102.
9 **Pacejka, H. B.** and **Sharp, R. S.** Shear force development by pneumatic tyres in steady state condition: a review of modelling aspects. *Veh. Syst. Dynamics*, 1991, **20**, 121–176.
10 **Pacejka, H. B.** and **Bakker, E.** The Magic Formula tire model. *Veh. Syst. Dynamics*, 1993, **21**, 1–18.
11 **Allen, R. W., Christos, J. B.** and **Rosenthal, T. J.** A tire model for use with vehicle dynamics simulations on pavement and off-road surfaces. *Veh. Syst. Dynamics*, 1997, **27**, 318–321.
12 **Allen, R. W., Magdaleno, R. E., Rosenthal, T. J., Klyde, D. H.** and **Hogue, J. R.** Tire modelling requirements for vehicle dynamics simulations. SAE Technical paper 950312, 1995, pp. 95–115.
13 **Xia, X.** and **Willis, J. N.** The effect of tire cornering stiffness on vehicle linear handling performance. SAE Technical paper 950313, 1995, pp. 117–126.
14 **Kortüm, W.** and **Sharp, R. S.** *Multi-body Computer Codes in Vehicle System Dynamics*, 1973 (Swets und Zeitlinger, Amsterdam).
15 **Kortüm, W.** and **Schiehlen, W.** General purpose vehicle system dynamics software based on multi-body formalisms. *Veh. Syst. Dynamics*, 1985, **14**, 229–263.
16 **Kübler, R.** and **Schiehlen, W.** Vehicle modular simulation in system dynamics. In Transactions of IMechE Conference on *Multi-body Dynamics: New Techniques and Applications*, London, 1998, paper C553/039/98, pp. 249–258.
17 *ADAMS/Tyre User's Guide—Version 5.2*, October 1987 (Mechanical Dynamic Inc.).
18 **Rahnejat, H.** *Multi-body Dynamics: Vehicles, Machines and Mechanisms*, July 1998 (Professional Engineering Publishing, Bury St Edmunds, UK; Society of Automotive Engineers, Warrendale, Pennsylvania, USA).
19 **Gear, C. W.** Simultaneous numerical solution of differential-algebraic equations. *Circuit Theory*, 1971, **18**, 89–95.
20 **Gear, C. W.** The numerical solution of problems which may have high frequency components. In Proceedings of NATO ASI on *Computer Aided Analysis and Optimization of Mechanical System Dynamics*, 1984 (Springer-Verlag).
21 British Standard Automobile Series, BS AU 230, Lateral transient response behaviour of passenger cars, 1989 (British Standards Institution).

View publication stats